Experimental and theoretical studies of the quenching of Li (3p , 4p) by N2

Vivek Komaragiri, Benjamin Mccarter, Solomon Bililign, Denis Hagebaum-Reignier, Vincent Ledentu, Gwang-Hi Jeung

Experimental and theoretical studies of the quenching of Li($3p$,$4p$) by N_2

Vivek Komaragiri, Benjamin McCarter, and Solomon Bililign[a)]
Department of Physics, North Carolina Agricultural and Technical State University, Greensboro, North Carolina 27411

Denis Hagebaum-Reignier, Vincent Ledentu, and Gwang-Hi Jeung[b)]
Chimie Théorique, Université de Provence, Case 521 [Consiglio National de la Recherche. Scientifique (CNRS) Unite Mixte de Recherche (UMR) 6517], Campus de St-Jérôme, 13397 Marseille Cedex 20, France

(Received 19 April 2005; accepted 13 June 2005; published online 18 July 2005)

Quenching mechanisms of the Li($3p$) and Li($4p$) states in collision with the nitrogen molecule are studied by laser-induced fluorescence spectroscopy and by a quantum chemical calculation. The Li($3p$) state is observed to be efficiently quenched to the Li($3s$) state detected as intense $3s \rightarrow 2p$ emission. The Li($4p$) state is efficiently quenched to the Li($4s$) and Li($3d$) states detected as $4s$-$2p$ and $3d$-$2p$ emissions, respectively. The potential-energy surfaces for the Li($2s$-$4p$)N_2 states show a large number of conical intersections and avoided crossings resulting from the couplings between the ionic $[Li^+(N_2)^-]$ and covalent configurations. There are a large number of stable excited states, and we give here the spectroscopic constants for the lowest two stable isomers correlating to Li($2p$)+N_2. © *2005 American Institute of Physics*. [DOI: 10.1063/1.1993588]

I. INTRODUCTION

Energy transfer in collisions between excited-state alkali-metal atoms and rare-gas atoms as well as the nonreactive quenching of excited alkali atoms by small molecules have been subjects of great interest.[1–10] For lithium, we have conducted several experimental and theoretical studies[11–15] involving energy transfer and reactions of excited states of Li by atoms and small molecules. We have measured[16] the cross sections and absorption profiles of the collisions of Li(np) by several alkane and alkene hydrocarbons (CH_4,C_2H_4,C_2H_6, and C_3H_8). This work showed that the internal structure of the perturber is important in the interpretation of an absorption profile.

Furthermore, in spite of the large cross section for quenching of Li by CH_4,C_2H_6, and C_3H_8, the LiH formation is not an important channel and it appears that efficient electronic to vibrational, rotational, and translational energy transfer is the main quenching channel. Only the collision with C_2H_4 is found to lead to the LiH formation.[15]

In comparison to earlier studies, N_2 is a challenging molecule since a stable complex (in the ground or excited states) can be formed as a result of mixture of ionic and covalent configurations. The nitrogen molecule is known to be the most stable dimer (homopolar diatomic molecule). This molecule uses three most efficient bonds, one σ bond made from $2p_\sigma$ hybrid atomic orbitals (AOs) and two π bonds made from bonding p_π AOs. The interaction between this very compact closed-shell structure and a metal atom can be understood in analogy with the rare-gas atom interacting with a metal atom, for example. In this case, the only significant interaction would consist of two terms: (1) the steric repulsion between the closed-shell electron distribution of the nitrogen molecule and the diffuse metal valence electron distribution and (2) the effective charge/induced dipole interaction term. However, one has to include the coupling with the ionic interaction term between the metal cation and the anion of the nitrogen molecule. On first thought, we might discard this third term at least for the ground state because the nitrogen molecule is known to have a large negative electron affinity because the supplementary electron should mainly stay in the π_g antibonding molecular orbitals (MOs). Contrary to this expectation, we are going to show in this work that only the ionic configuration, $Li^+(N_2)^-$, leads to a stable bound state.

A model theoretical study of the electronic states of LiN_2 was done by Sevin *et al.*[16,17] in the late 1980s using an interesting valence-bond analysis for the ionic and covalent avoided crossings in the LiN_2 complex. Although this study showed conceptually valid aspects, the limited accuracy of their method of computation and the absence of the long-range part of the potential-energy surfaces (PESs) required more up-to-date, accurate, and extended calculations. The general problem of the accuracy concerning the molecules containing a pair of a donor-acceptor has been analyzed in a recent study by Jeung.[18] That work showed an interesting picture of the interplay between the ionic configuration and the neutral (or covalent) configuration in the diatomic molecules.

In Sec. II of this work the "half-collision" pump-probe technique is used. This technique has been used to measure the continuum or "scattering state" absorption profiles of several collision complexes.[6–8,11–13] This method has proved its usefulness to study the molecular dynamics for a number of metal-atom reagents,[6,7,10–15] where the pump laser excites the transient collision complex directly from the ground state to an excited one. This technique allows a selective excita-

[a)]Electronic mail: bililign@ncat.edu
[b)]Electronic mail: jeung@up.univ-mrs.fr

tion of states of well-defined symmetry in the collision complex. Final state-resolved measurements of the far-wing action spectra are sensitive to both the shape of the PES in the entrance channel and to the subsequent dynamical evolution of the excited state. This provides information on nuclear reaction dynamics, nonadiabatic interactions, and the effect of reagent electronic orbital alignment on the final state branching and energy disposal.

Theoretical *ab initio* methods are used to calculate the LiN_2 potentials and interpret the results of experimental studies of inelastic collisions of $Li(np, n=3,4)+N_2$, represented as

$$Li(2s) + N_2 + h\nu \Rightarrow [Li(np, n = 3,4)N_2]^* \Rightarrow Li(np) + N_2 \quad (1a)$$

$$\Rightarrow Li(ns, n = 3,4) + N_2 \quad (1b)$$

$$\Rightarrow Li(3d) + N_2. \quad (1c)$$

II. EXPERIMENTAL DETAILS

The details of the experimental setup have been described in previous works.[6,7,10–15] Briefly, the doubled and tripled frequencies of a 20-Hz Nd: yttrium aluminum garnet (YAG) laser were used to pump two dye lasers simultaneously in a laser pump-probe arrangement. Only the pump laser was used for the inelastic collision studies. The pump dye laser was operated using a dicyanomethylene (DCM) dye whose output was frequency doubled to the spectral region of the $Li(3p \leftarrow 2s)$ resonance transition at 323.3 nm and fluorescein dye whose output was frequency doubled to the spectral region of the $Li(4p \leftarrow 2s)$ second resonance transition at 274 nm. The pump-laser pulse had a typical pulse width of 4-6 ns and pulse energy between 50 and 100 μJ. This output was focused to the center of a five-arm stainless-steel heat pipe oven containing Li vapor and the quenching gas N_2, at an oven temperature of 900 K, corresponding to a Li atom vapor density of $\sim 10^{13}/cm^3$. The typical operating pressure of the buffer gas was 6–8 Torr, and the pressure was measured with a capacitance manometer.

For the resonance excitation to measure the cross sections, the laser was tuned to the $Li(3p\ ^2P_{3/2} \leftarrow 2s\ ^2S_{1/2})$ transition at 323.3 nm, and the output was focused to the center of a stainless-steel heat pipe oven containing Li and quenching gases at 573 K. The sensitized fluorescence of the Li $(3s \rightarrow 2p)$ atomic transition at 812.6 nm was measured as a function of gas pressure from 1 to 9 Torr.

The direct atomic fluorescence from the laser excited $Li(4p)$ or $Li(3p)$ states to the ground state is very weak due to a heavy radiation trapping and it was experimentally difficult to resolve the atomic fluorescence from the scattered near-resonant pump-laser light. The nonreactive profile for $Li(3p)$ was determined indirectly by monitoring the cascade fluorescence on the $Li(3s \rightarrow 2p)$ atomic transition at 812.6 nm. The temporally integrated signal intensity is then measured as a function of detuning of the laser in the red and blue wings of the $Li(3p \rightarrow 2s)$ transition.

Similarly for the $Li(4p)$ studies, we chose to do the measurement indirectly by monitoring the cascade fluorescence of the $Li(4s \rightarrow 2p)$ transition at 492 nm and the $Li(3d \rightarrow 2p)$ transition at 610 nm. The temporally integrated signal intensity is then measured as a function of detuning of the laser in the red wing of $Li(4p \rightarrow 2s)$ transition. No attempt was made to detect $Li(3s \rightarrow 2p)$ fluorescence following the $Li(4p \leftarrow 2s)$ excitation.

In these experiments we believe that the $3s, 4s$, and $3d$ states are predominantly populated through collisional quenching of the LiN_2 complex, even though we cannot rule out the possibility that the $3s$ or the $4s$ and $3d$ states might also be populated by fluorescence from the $Li(3p)$ or $Li(4p)$ states, respectively. However, such spontaneous emissions involving relatively small energy differences should be far less intense in comparison with the collisional energy transfers.

The fluorescence from these states was collected using a lens and a steering mirror assembly by a 35-cm McPherson model 2035 monochromator with a 1200-lines/mm holographic grating operated with wide slits. The fluorescence was detected with a photomultiplier, and the signal output was amplified using a fast preamplifier and analyzed using a gated integrator/boxcar averager system. For the quenching cross-section studies, a 10-ns detection gate was scanned over the 0–300-ns range after the laser fired. Because of the finite laser pulse width, the detection system rise time, and gate width, the temporal resolution was limited to $\sim$10 ns. For the line-shape and reactive collision studies, the gate width was increased to 100 ns to give a temporally integrated signal. The pump-laser intensity was monitored with an energy meter and the far-wing profiles were normalized to constant incident energy.

Nonlinear processes in general may lead to strong photoionization, self-focusing, parametric amplification, and stimulated atomic emission processes. These problems are more significant near the line center (resonance), at high pump-laser power and high temperatures. We found out that the pump-laser energy should be extremely low in order to avoid multiphoton absorption. In the cross-section studies, the signals were linear in laser intensity and stimulated emission effects were ruled out. In fact, at higher laser powers and higher temperatures we observed very strong "fluorescence" signals from $Li(3s)$ with rapid rise and fall times which were independent of gas pressure, indicating the presence of a strong stimulated emission. We have verified that the Li^* signals are linear in the pump-laser beam intensity, by measuring the fluorescence as a function of pump-laser energy at different detunings, both near the line center and in the wings. We also measured the fluorescence signals as a function of perturber pressure in the range of 1–9 Torr, and they were linear, indicating that secondary collisions could be ruled out under the conditions of our experiment.

III. EXPERIMENTAL RESULTS

The collisional energy-transfer processes from $Li^*(3p) + N_2$ collisions were investigated under gas cell conditions by monitoring the $Li(3s \rightarrow 2p)$ far red-wing and blue-wing absorption profiles. Similarly, the $Li^*(4p) + N_2$ collisional energy-transfer processes were studied by detecting the

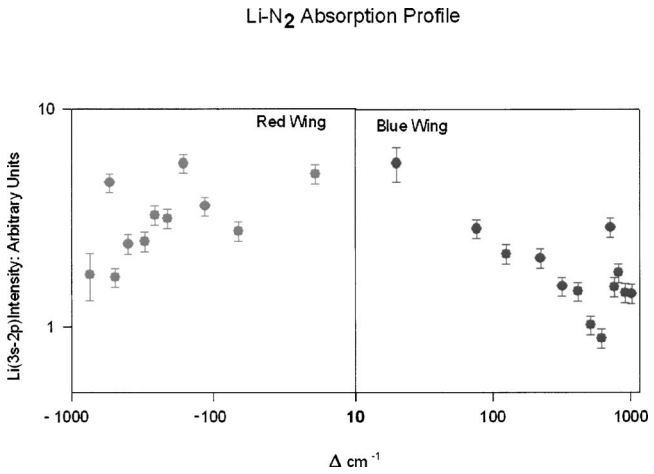

FIG. 1. A log-log plot of the experimental far red-wing and blue-wing absorption profiles for the Li(3p)N_2 complex: Nonreactive Li(3$s \rightarrow 2p$) fluorescence signal as a function of pump-laser detuning ($\Delta = \omega_L - \omega_o$) from Li(3$p \leftarrow 2s$) atomic resonance transition.

Li(4$s \rightarrow 2p$) and the Li(3$d \rightarrow 2p$) fluorescences. The blue-wing excitation to the Li(4p) state can also populate the Li(4d) and Li(4f) states which are close to the Li(4p) state. Because of this and other experimental difficulties we were unable to measure the blue-wing profiles for the Li(4p) studies.

Figure 1 shows the relative population in the nonreactive product channel corresponding to process (1b), for $n=3$ in the red and blue wings. The profiles in each case are averaged over several runs and normalized to a constant incident energy.

We show in Fig. 2 the relative populations of the nonreactive product channel corresponding to the process (1b) for $n=4$ and process (1c) in the red wing. Figure 3 shows the intensity ratio of the Li(3$d \rightarrow 2p$) fluorescence to the Li(4$s \rightarrow 2p$) fluorescence.

Since the radiative lifetime for the Li(3s) state is seven

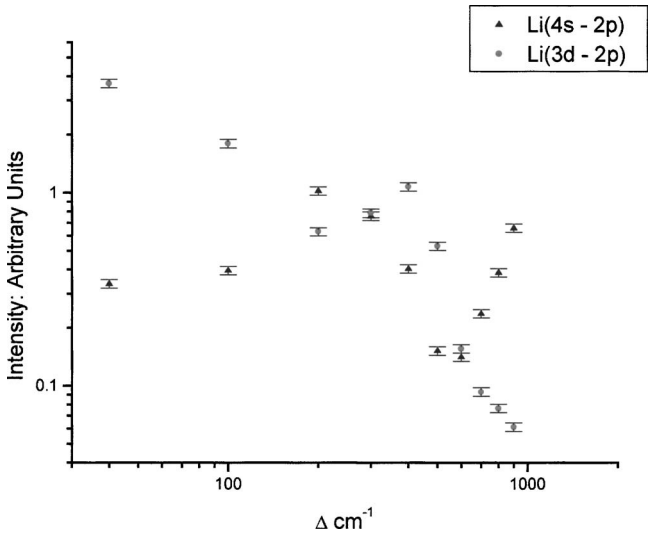

FIG. 2. A log-log plot of the experimental far red-wing absorption profiles for the LiN_2 complex: Nonreactive Li(4$s-2p$) fluorescence signal (▲) and the Li(3$d \rightarrow 2p$) fluorescence signal (●) as a function of pump-laser detuning ($\Delta = \omega_L - \omega_o$) from the Li(4$p \leftarrow 2s$) atomic resonance transition.

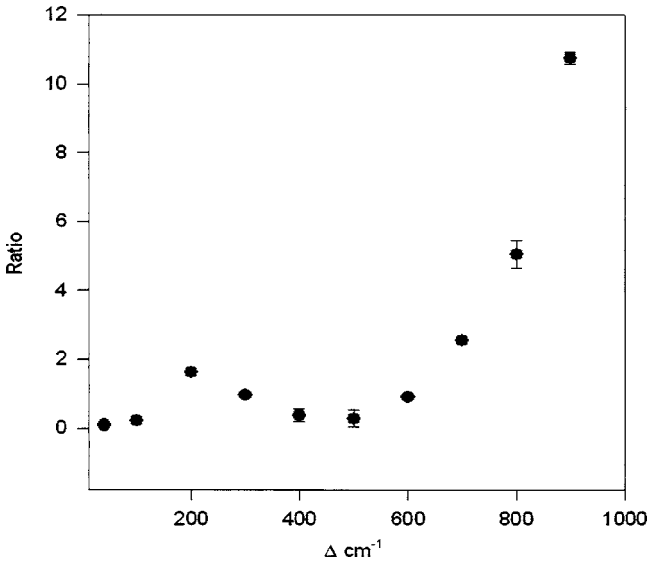

FIG. 3. The ratio of the Li(3$d \rightarrow 2p$) to Li(4$s \rightarrow 2p$) experimental far red-wing absorption as a function of pump-laser detuning ($\Delta = \omega_L - \omega_o$) from the Li(4$p \leftarrow 2s$) atomic resonance transition. Note: the ratio is on a linear scale and Δ is on a log scale.

times shorter than the Li(3p) state, the pressure dependence of the time constant Ω_1 (which is the sum of the spontaneous emission rate and the collision-induced deactivation rate) for the Li(3p) state can be obtained by analyzing the cascade fluorescence time profiles at low pressure of Li(3s). Then, the radiative lifetime and the total quenching cross section for the Li(3p) state can be obtained. The model developed in our earlier work[15] has been used to extract the quenching cross section for Li(3p)+N_2 to be 27.0±2.7 Å^2, which is comparable to that for C_2H_4. However, the quenching cross section for Li(3p)+H_2 is found to be 2.3±1.0 Å^2, a much smaller value. The large cross section of Li(3p)+N_2 is consistent with the stronger signal in the absorption profile for this system compared to our earlier result of the Li(3p)–H_2 profile. The large difference in the cross sections between Li–N_2 and Li–H_2 is consistent with the results of the cross sections of the first excited ^2P states of LiN_2 and LiH_2.[19]

IV. THEORETICAL METHOD

First, we have optimized 12s8p5d Gaussian-type orbitals (GTOs) to represent the 2$s-4d$ states of the lithium atom and 12s7p3d GTOs for the neutral and anionic ground states of nitrogen atom. Those functions were used without contraction for the atomic basis functions (ABFs). The complete active space (CAS) self-consistent-field (SCF) method was used to get the state-averaged MOs. Then the multireference (MR) configuration-interaction (CI) calculation was done. We have used different levels of calculation to study the PESs. First, a low-level method was used to explore the PESs. Here, only one radical electron was distributed in the active MOs in all possible ways for the given point-group symmetry, apart from the six other valence electrons (three from each nitrogen atom) which were kept in three paired closed shells. For the MRCI calculation, only single substitution was allowed from the six electrons. The active space consists of all MOs originating from the 2s-4p AOs of

lithium. The total numbers of the configuration state functions (CSFs) so generated are tens of thousands. This method is not sufficiently accurate to obtain reliable PESs although the qualitative features (the presence of conical intersections and avoided crossings between the PESs) remain unchanged in higher-level calculations. In the second method, double substitutions were allowed for the six electrons, which makes the total number of CSFs on the order of from hundreds of thousands to one million. This method is more suitable for quantitative study of the ground and excited states up to $Li(4p)N_2$.

The third method was used for the linear ($C_{\infty v}$) and C_{2v} geometries, where the active space was reduced to seven MOs originating from $2s$ and $2p$ AOs of lithium atom (four) and the σ_g and π_u MOs from the nitrogen molecule (three), but the seven electrons were to be distributed in the active space in all possible ways, and all single and double substitutions from this reference space were included. This makes the total number of CSFs very large, on the order of several millions (e.g., 3 174 702 for the $^2B_1$ states, and 3 203 830 for the $^2\Sigma^+$ states). Although this method should give the most accurate representation for the $Li(2s)N_2$, the $Li(2p)N_2$, and the ionic states, it cannot appropriately describe higher states. This method was used to characterize the two lowest stable isomers which correlate to $Li(2p)N_2$ [the lowest state corresponding to $Li(2s)N_2$ has only a weak van der Waals attraction].

In the first series of calculations, the N-N distance was kept at 2.08 bohrs which is longer than our SCF calculated ground-state bond distance of the free N_2 molecule, 2.01 bohrs [the experimental value is 2.074 bohrs (Ref. 20)], but shorter than our CAS SCF calculated bond distance of $(N_2)^-$, 2.18 bohrs. Then the N-N distance was varied to find the minimum energy and the corresponding geometry of the LiN_2 complex. The MOLCAS program package[21] was used in the molecular calculations.

The PESs of the stable bound states of LiN_2 complex near the minimum-energy region have been fitted by fifth-order polynomial functions and two vibrational frequencies, equivalent to the symmetric-stretching frequency (ν_1) and the bending frequency (ν_2), have been calculated. The rms errors for the fitting were less than 4×10^{-4} hartree for the linear ($C_{\infty v}$) case and less than 2×10^{-5} hartree for the C_{2v} case.

V. THEORETICAL RESULTS

The C_{2v} section of the PESs for the A_1 and B_1 states transforming to the A' states in the C_s symmetry and corresponding to the $Li(3p,3d,4s,4p)$ asymptotes for large Li-N_2 distances is presented in Fig. 4. The data for this figure were obtained with the second method of calculation. These PESs show many crossing surfaces where the crossing points represent conical intersections. There are also several avoided crossing surfaces originating from the couplings between the ionic and the covalent configurations. This aspect also exists in other sections (linear and C_s) of the PESs. A physical consequence of these crossing and avoided-crossing PESs is a large probability of transition between different

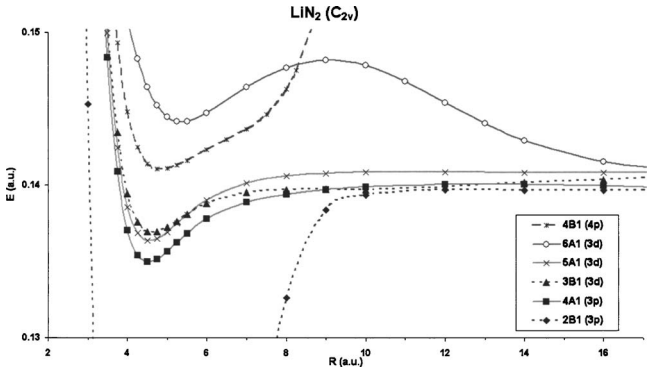

FIG. 4. A C_{2v} section [with the r(N-N) distance fixed to 2.08 bohrs] of the A' potential-energy surfaces of the LiN_2 complex where R is the distance between the lithium atom and the midpoint of the two nitrogen atoms (in a. u.). The corresponding asymptotes for large R are put inside the parentheses following the state designation. The energy (E) is with respect to the $Li(2s)+N_2$ asymptote.

PESs. For example, the LiN_2 complex in an initial state correlating with $Li(4p)$ would easily quench in to a state correlating to $Li(4s)$ via the $4\,^2B_1$ to $7\,^2A_1$ transition around a conical intersection at around 15 bohrs (far higher in energy than in Fig. 4) or quench into a state correlating with the $Li(3d)$ state via the $4\,^2B_1$ to $6\,^2A_1$ transition around a conical intersection at around 8 bohrs appearing in Fig. 4. The lower $Li(3d)$ states ($5\,^2A_1$ or $3\,^2B_1$) would easily transform to the $Li(3p)$ states ($4\,^2A_1$ or $2\,^2B_1$) via two conical intersections (around 6 and 9 bohrs) and via an avoided-crossing region (around 10 bohrs), both shown in Fig. 4. The $Li(3p)$ state itself meets the conical intersection with the $Li(3s)$ surface ($2\,^2A_1$), so this quenching should also be a highly probable process.

In our previous studies on the Li/rare-gas, LiH_2, and $LiCH_4$ systems we did not see so many conical intersections [except between the electronic states originating from the $Li(2p)$ and $Li(3s)$ states] nor the ionic-covalent avoided crossing. Thus, we expect the emission spectra of this LiN_2 complex to be very different from those previous cases. In particular, we can expect a larger number of quenching processes and higher probabilities for the corresponding radiationless energy conversions.

Another consequence of the ionic-covalent coupling is the changing nature of the LiN_2 complex as a function of the Li-N_2 distance (R). For the linear case, e.g., the $^2\Pi$ states include important ionic contributions while the $^2\Sigma^+$ states and the $^2\Delta$ states do not. The lowest (1) $^2\Pi$ state is ionic at short Li-N (the nitrogen atom in immediate contact with the lithium atom) distances, the second (2) $^2\Pi$ state is ionic for larger Li–N distances, and the third (3) $^2\Pi$ state is ionic for still larger Li-N distances, etc. The ionicity (i.e., the magnitude of the dipole moment or the effective charge of the lithium atom) of these complexes increases from the $1\,^2\Pi$ state to the $3\,^2\Pi$ state. These two aspects are exactly the same as in the polar diatomic molecules.[2] Figure 5 shows some of the potential-energy curves in the linear case. Here, the energies were calculated by the third method. The lowest electronic energy of the $1\,^2\Pi$ state is 0.980 eV higher than the dissociation limit into $Li(2s)+N_2$. The crossing point between the $^2\Sigma^+$ and the $^2\Pi$ states for a given r(N-N) distance

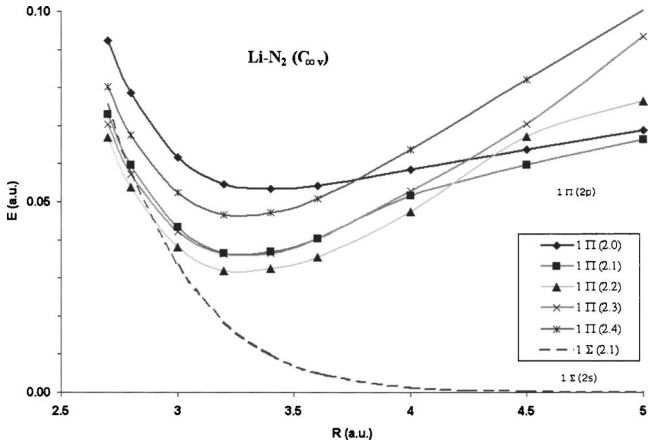

FIG. 5. A linear section of the potential-energy surfaces of the Li-N_2 complex showing the lowest two states ($1\ ^2\Sigma^+$ and $1\ ^2\Pi$) where R is the distance between the lithium atom and the nitrogen atom in direct contact with the lithium atom and the numbers in parentheses are the r(N-N) distances (in a. u.). The energy (E) is with respect to the Li($2s$)+N_2 asymptote.

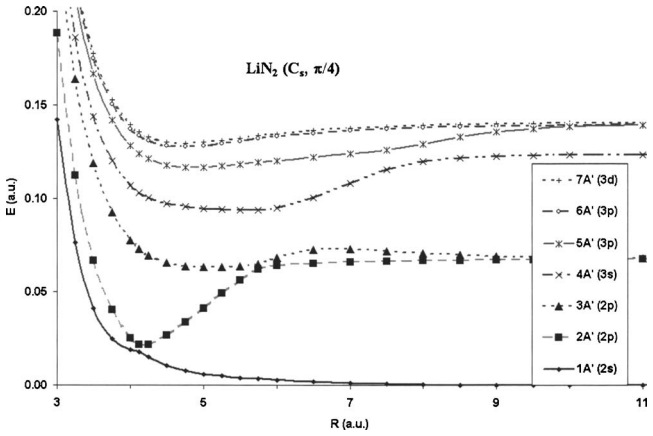

FIG. 6. A C_s section [with the r(N-N) distance fixed to 2.08 bohrs] of the potential-energy surfaces of the Li-N_2 complex, where R is the distance between the lithium atom and the midpoint of the two nitrogen atoms and the nitrogen molecular axis makes a $\pi/4$ angle with the R axis (in a. u.). The energy (E) is with respect to the Li($2s$)+N_2 asymptote.

represents a conical intersection. We can see one conical intersection between the $1\ ^2\Sigma^+$ state and the $1\ ^2\Pi$ state for $r=2.1$ at R(Li–N)$\approx$2.8. The set of these conical intersections as the r(N-N) is varied represents the seam line between those two states. The radiationless transition between those two states should occur preferentially around this seam line.

In the C_{2v} case, the $^2B_1$ states show a strong ionicity, the $1\ ^2B_1$ state at short intermolecular distances, the $2\ ^2B_1$ state at a medium range, and the $3\ ^2B_1$ state at a longer range. The $^2A_1$ states are covalent in nature. Here again the crossing points between two different point groups are conical intersections. The lowest conical intersection shows a far larger activation barrier for the addition reaction than in the linear case. Thus the addition reaction should occur preferentially through the linear geometry. The lowest stable state of the C_{2v}LiN$_2$ complex is the $1\ ^2B_1$ state but the minimum energy of this state is 1.263 eV higher than the minimum energy of Li($2s$)+N_2. So, the lowest stable geometry of the LiN$_2$ complex appears to be a linear Li-N-N one. The corresponding equilibrium geometry of the $1\ ^2B_1$ state shows the Li-N distance of about 3.4 bohrs and the N-N distance of about 2.2 bohrs, which is practically equal to the bond distance of the free anion of nitrogen molecule calculated in a SCF calculation (see Sec. IV). The Mulliken charge, which gives approximate estimation of the effective charge but is not an observable, is 0.63 for lithium. However, the dipole moment, which is an observable, is calculated to be 2.3833 a.u. If we divide this by the Li-N_2 distance, we obtain the effective charge of 0.70, which is slightly larger than the Mulliken charge.

Figure 6 shows the $^2A'$ states of C_s symmetry making a cascade of avoided crossings (the data for this figure were obtained with the first method of calculation). The energetically lowest one occurring at short (around 4 bohrs) Li-N_2 distances involves the neutral Li($2s$)+N_2 and the ionic $Li^+ + (N_2)^-$ configurations. The second lowest avoided crossing occurring at around 5.75 bohrs involves the ionic configuration and one of the two Li($2p_\parallel$)+N_2 configurations where $2p_\parallel$ means a linear combination of the two $2p$ angular momentum eigenfunctions parallel to the molecular plane. [The $1\ ^2A''$ state should be Li($2p_\perp$)+N_2 with this notation.] The other Li($2p_\parallel$)+N_2 configuration is involved in an avoided crossing with the ionic configuration near 6.5 bohrs with a large splitting. The fourth avoided crossing occurring at around 8 bohrs concerns the ionic configuration and the Li($3s$)+N_2 configuration, and so forth. We can see in Fig. 6 that the $^2A'$ state has a stable potential well due to an avoided crossing between the two lowest $^2A'$ states. In fact, most of the excited states have stable potential wells representing excited complexes (or exciplexes).

The spectroscopic calculations for the $1\ ^2\Pi$ state and the $1\ ^2B_1$ state are reported in Table I. The N-N vibrational frequencies are significantly smaller than in the free nitrogen molecule, 2359 cm^{-1},[20] suggesting a large perturbation by the alkali atom. This frequency shift is larger for the linear case with respect to the C_{2v} case. This is in agreement with the bond strength: the linear complex is indeed more strongly bonded than the C_{2v} isomer.

Among the covalent electronic states, some states have the metal electron distributed along the metal-N_2 intermolecular region. That is the case for the covalent $^2\Sigma^+$ states, the $^2A_1$ states, and the $^2A'$ states originating from Li(ns) and the highest Li(np) and Li(nd) states. Those states show a long-range potential maxima (more precisely, a local maxima). The physical origin of those local maxima was explained before.[22] The potential maxima can be correlated to the behavior of the blue-wing spectra because the excitation frequency should coincide with the difference between

TABLE I. The equilibrium interatomic distances (in Å) and two vibrational frequencies (in cm^{-1}) for the linear ($C_{\infty v}$) and C_{2v} isomers of the lowest bound stable LiN$_2$ complex.

	Linear	C_{2v}
r(N-N)	1.164	1.167
R(Li-N)	1.736	1.796
ν(N−N)	1880	1942
ν(Li-N_2)	756	680

the excited-state energy and the ground-state energy. However, we do not attempt here to give a reasonable explanation for the blue-wing spectra as many more factors intervene in this area.

Our results show why we need to survey the PESs covering a wide range of intermolecular distances and also a wide range of electronic energy to fully understand the meaning of the ionic-neutral couplings. The consequence of the consecutive ionic-neutral couplings is the efficient quenching of the $^2A'$ electronic states. The most efficient quenching processes should occur around the linear and C_{2v} conical intersections because the collision energy can most easily bring about nonadiabatic transitions there.

VI. DISCUSSIONS

It is understandable that metal complexes with halogen or oxygen molecules are stable and bound because the electron affinities of those diatomic species are large and positive. However, the electron affinity of the N_2 molecule is known to be negative: −1.8 eV according to an experimental data[23] and −1.57 eV according to our calculation. So it is surprising that the nitrogen molecule can make such a strong stable bond with the lithium atom. The presence of the Li cation should play a largely stabilizing role in this complex.

It is generally agreed that in the Born-Oppenheimer/Franck-Condon approximation, there is often a simple relationship between the laser detuning (Δ) and the Condon point (R_c), the internuclear separation where excitation occurs. In the long-range van der Waals region the Condon point can be determined if the C_6 coefficients of the ground [Li($2s$)–N_2] and Li($3p$)–N_2 are known. The C_6 coefficient[24] for the Li($2s$)–N_2 is found to be 1.71×10^{-58} erg Å^6. From our measured quenching cross section of Li($3p$) by N_2 and using the simple orbiting model formula[15] relating the C_6 coefficient to the cross section we estimated the C_6 coefficient for Li($3p$)–N_2 to be 3.41×10^{-58} erg Å^6. We can correlate the detuning frequency range probed in this experiment which is $20\leqslant\Delta\leqslant700$ cm^{-1} in the red wing and $20\leqslant\Delta\leqslant1000$ cm^{-1} in the blue wing to the probed internuclear distance range which is 7.39 Å$\geqslant R_c\geqslant$4.22 Å in the red and 7.39 Å$\geqslant R_c\geqslant$3.95 Å in the blue.

The red-wing absorption in Fig. 1 corresponds to the excitation from the largely repulsive ground-state PES to the attractive PES originating from the Li($3p$)+N_2 asymptote, i.e., the 2 $^2B_1$,4 $^2A_1$, and 3 $^2B_1$ states; or the 2 $^2\Pi$ and 4 $^2\Sigma^+$ states; or more generally the 5 $^2A'$6 $^2A'$, and 7 $^2A'$ states. Free-free excitation can be included at small detunings. However, the free-bound transition is the dominant absorption process as the detuning increases. We see a decreasing $3p-3s$ quenching rate as the detuning increases. This quenching should happen through the conical intersection between the largely attractive PES (the 2 $^2B_1$ or 2 $^2\Pi$ state) and a weakly attractive PES (the 3 $^2A_1$ or 3 $^2\Sigma^+$ state), and also through an avoided crossing between the 4 and 5 $^2A'$ PESs (Fig. 6). Since we are measuring the cascade fluorescence of the Li($3s-2p$) transition following excitation to the Li($3p$)+N_2 state, the increased intensity and presence of prominent satellite structures in the red wing corresponding to large detuning (short internuclear distance) may result from the transition around the conical intersection at relatively long Li-N_2 distances (around 7 bohrs for the linear and C_{2v} cases).

The overall intensity of the blue-wing profile is smaller than the red-wing intensity beyond 100 cm^{-1} and falls off more rapidly. With increasing collision energy the lifetime decreases rapidly, which may explain the large transition rate near the line center and a decreasing rate as the detuning increases. We cannot explain the increase in the intensity and the satellite at large detuning in the blue wing. There is no evidence of a barrier in the 4 $^2A_1$ state, which could explain the satellite.

The dominant process for the Li($4p$)+N_2 quenching should be the surface hopping from the 4 $^2B_1(4p)$ to the 7 $^2A_1(4s)$ surface and from the 4 $^2B_1(4p)$ to the 6 $^2A_1(3d)$ surface.

VII. CONCLUSION

Contrary to our previous studies, the interaction between the lithium atom and the nitrogen molecule shows a strong interaction, which makes the potential-energy surfaces far more complex involving a large number of the conical intersections and avoided crossings. It is evident that the nitrogen molecule accepts the supplementary electron much more easily in the presence of the alkali atom to make stable ionic complexes than do the rare gases, H_2 and CH_4. In this regard, the nitrogen molecule acts similar to the halogen molecules, although the ground state of the alkali/N_2 complex is repulsive. In particular, the lowest stable complex, which is ionic around its equilibrium geometry, is made from the lowest of a cascade of the ionic-covalent avoided crossing surfaces. The physical consequence of the excitation of this complex is a very efficient quenching of the initial state through successive radiationless transitions. Concerning a quantitative interpretation of the observed emission spectra, one has to do a quantum scattering calculation starting from a vast domain of the potential-energy surfaces.

ACKNOWLEDGMENTS

We (S.B., V.K., and B.McC.) gratefully acknowledge the financial support of the National Science Foundation (CHE-0131115). The theoretical part has been supported by the CNRS. We give special thanks to Professor T. R. Sandin for kindly reading the manuscript.

[1] W. H. Breckenridge and H. Umemoto, Adv. Chem. Phys. **50**, 213 (1992).
[2] L. Krause, Adv. Chem. Phys. **28**, 267 (1975).
[3] E. E. Nikitin, Adv. Chem. Phys. **28**, 317 (1975).
[4] T. F. Gallagher, W. E. Cooke, and S. A. Edelstein, Phys. Rev. A **17**, 125 (1978); N. Allard and J. Kielkopf, Rev. Mod. Phys. **54**, 1103 (1982).
[5] I. V. Hertel, Adv. Chem. Phys. **50**, 475 (1982).
[6] S. Bililign, P. D. Kleiber, W. R. Kearney, and K. M. Sando, J. Chem. Phys. **96**, 218 (1992); Phys. Rev. A **42**, 6938 (1990).
[7] S. Bililign and P. D. Kleiber, J. Chem. Phys. **96**, 213 (1992); P. D. Kleiber, T. H. Wong, and S. Bililign, *ibid.* **98**, 1101 (1993).
[8] W. H. Breckenridge and H. Umemoto, in *The Dynamics of the Excited State*, edited by K. Lawley (Wiley, London, 1982); W. H. Breckenridge, in *Reactions of Small Transient Species*, edited by M. Clyne and A. Fontijin (Academic, London, 1983); J. Chem. Phys. **100**, 14840 (1996).
[9] W. H. Breckenridge and H. Umemoto, J. Chem. Phys. **75**, 698 (1981); J.

Chem. Phys. **77**, 4464 (1982); **81**, 3852 (1984).
[10] P. D. Kleiber, in *Chemical Dynamics and Kinetics of Small Radicals*, edited by K. Liu and A. Wagner (World Scientific, Singapore, 1996); P. D. Kleiber, W. C. Stwalley, and K. M. Sando, Annu. Rev. Phys. Chem. **44**, 13 (1993).
[11] S. Bililign, B. C. Hattaway, N. Geum, and G.-H. Jeung, J. Phys. Chem. A **104**, 9454 (2000).
[12] S. Bililign, B. C. Hattaway, T. L. Robinson, and G.-H. Jeung, J. Chem. Phys. **114**, 7052 (2001).
[13] S. Bililign, B. C. Hattaway, and G.-H. Jeung, J. Phys. Chem. A **106**, 222 (2002).
[14] J. T. Swindell II, B. McCarter, V. Komaragiri, and S. Bililign, Chem. Phys. **305**, 299 (2004).
[15] B. Hattaway, S. Bililign, L. Uhl, V. Ledentu, and G.-H. Jeung, J. Chem. Phys. **120**, 1739 (2004).
[16] A. Sevin, C. Giessner-Prettre, P. C. Hiberty, and E. Noizet, J. Phys. Chem. **95**, 8580 (1991).
[17] A. Sevin, P. Chaquin, L. Hamon, and P. C. Hiberty, J. Am. Chem. Soc. **110**, 5681 (1988).
[18] G.-H. Jeung, Theor. Chem. Acc. (to be published).
[19] C. Bottcher and C. V. Sukumar, J. Phys. B **14**, 2853 (1977).
[20] Chemistry webbook of the NIST, http://webbook.nist.gov.
[21] K. Andersson, M. R. A. Blomberg, M. P. Fülscher *et al.*, MOLCAS, version 4, Lund University, 1997.
[22] A. Yiannopoulou, G.-H. Jeung, S. J. Park, H. S. Lee, and Y. S. Lee, Phys. Rev. A **59**, 1178 (1999).
[23] G. J. Schultz, Rev. Mod. Phys. **45**, 423 (1973).
[24] D. J. Margoliash and W. J. Meath, J. Chem. Phys. **68**, 1426 (1978).